Fundamental role of nonlocal orders in 1D extended Bose–Hubbard model

Chaos
An Interdisciplinary Journal of Nonlinear Science

RESEARCH ARTICLE | JUNE 05 2024

Fundamental role of nonlocal orders in 1D extended Bose–Hubbard model

Special Collection: Topics in Nonlinear Science: Dedicated to David K. Campbell's 80th Birthday

Nitya Cuzzuol ; Arianna Montorsi

Chaos 34, 063116 (2024)
https://doi.org/10.1063/5.0206798

Fundamental role of nonlocal orders in 1D extended Bose–Hubbard model

Cite as: Chaos 34, 063116 (2024); doi: 10.1063/5.0206798
Submitted: 4 March 2024 · Accepted: 14 May 2024 ·
Published Online: 5 June 2024

Nitya Cuzzuol[a] and Arianna Montorsi[b]

AFFILIATIONS

Institute for Condensed Matter Physics and Complex Systems, DISAT, Politecnico di Torino, I-10129 Torino, Italy

Note: This paper is part of the Focus Issue on Topics in Nonlinear Science: Dedicated to David K. Campbell's 80th Birthday.
[a]**Electronic mail:** nitya.cuzzuol@polito.it
[b]**Author to whom correspondence should be addressed:** arianna.montorsi@polito.it

ABSTRACT

Nonlocal order parameters capture the presence of correlated fluctuations between specific degrees of freedom, in otherwise disordered quantum matter. Here, we provide a further example of their fundamental role, deriving the ground state phase diagram of the filling one extended Bose–Hubbard model, exclusively in terms of their ordering. By means of a density matrix renormalization group numerical analysis, we show that in addition to the (even) parity order characteristic of the Mott insulating phase and the string order nonvanishing in the Haldane insulator, the recently proposed odd parity order completes the picture, becoming nonvanishing at the transition from the normal superfluid to the paired superfluid phase. The above three nonlocal parameters capture all the distinct phases, including the density wave phase, in which the local order is seen as the simultaneous presence of correlated fluctuations in different channels. They provide a unique tool for the experimental observation of the full phase diagram of strongly correlated quantum matter, by means of local density measurements.

The full phase diagram of the one-dimensional three-body constrained extended Bose–Hubbard (EBH) model is re-derived here solely in terms of three nonlocal order parameters (NLOPs), identified with the expectation values of appropriate disorder operators: the string operator and the even and odd parity operators. Their finiteness unveils the emergence of distinct correlated density fluctuations for each disordered phase, which can persist at non-zero temperatures, thanks to their nonlocal nature. These parameters can be detected by simple local density measurements in real experiments with quantum matter.

I. INTRODUCTION

The one dimensional 1D Hubbard model is the simplest paradigmatic model capturing the complex physics of strongly correlated particles (fermions or bosons) on a lattice. The model has been thoroughly studied in the last few decades. In particular, at integer fillings and low temperatures, for repulsive on-site density–density interaction U, a Mott insulating (MI) phase is observed, which escapes the Landau classification of spontaneous symmetry breaking (SSB) local orders.[1,2] Indeed, it has been shown that the phase is characterized by a nonlocal order in one dimension, known as the charge parity order in both bosonic[3] and fermionic[4] cases, whereas in two dimensions, it is captured by its generalization, namely, the brane parity order.[5] Despite their nonlocal nature, such orders are observed by local density measurements in atomic matter trapped onto optical lattices.[6–8] In fact, since they do not break any continuous symmetry, these orders persist at sufficiently low temperatures.

In the 1D fermionic extended Hubbard model,[9] the above MI phase is challenged by other insulating phases, which turn out to be associated with other types of nonlocal orders,[10,11] ultimately capturing the fundamental role of correlated quantum fluctuations in each of the possibly disordered distinct phases. The mathematical framework for nonlocal orders is provided by the concept of disorder operators,[12] which is not peculiar in insulating phases. Examples are the spin-parity order, observed in the Luther–Emery liquid phase of 1D fermions,[11] or the brane spin-parity, which is nonvanishing in the superconducting phase of the two dimensional (2D) case.[13] Most notably, in addition to parity orders, string nonlocal orders also appear in these systems, capturing symmetry protected topological (SPT) phases with nontrivial topological features.[14] This is the case of the Haldane phase, which can be observed in insulating

(HI) phases of bosons[10] and fermions,[11] as well as in conducting phases.[15,16] On more general grounds—at least for correlated spinful fermions in one dimension[17] described in the low energy limit by decoupled sine-Gordon models—the framework of SPT phases can be exploited to classify all distinct low temperature phases by means of appropriate nonlocal order parameters. In fact, taking advantage of such observations also for bosonic models, very recently, it has been shown that another type of charge parity order (named odd charge parity) is finite in the paired superfluid (PSF) phase of the Bose–Hubbard model.[18]

Here, we will explore the crucial role that nonlocal orders play in the full phase diagram of the extended Bose–Hubbard (EBH) model. Based on the theoretical framework, we will provide numerical evidence that the different possible correlated fluctuations shown in the right panel of Fig. 1 are, in fact, associated with three different nonlocal order parameters. Their finiteness uniquely identifies the disordered MI, HI, and PSF phases, as well as the locally ordered density wave (DW) phase. Each phase boundary is then identified by the vanishing of one of these operators, as shown in Fig. 1. Therefore, completeness of the phase separated (PS) region is also represented, which is not investigated here.

Our results, in addition to reinforcing evidence on the fundamental role of correlated fluctuations in disordered quantum matter, provide an immediate tool for the observation of these distinct phases by local density measurements in experiments at sufficiently low temperatures.

II. MODEL

We will focus onto the study of the 1D extended Bose–Hubbard model, which can be described by the Hamiltonian operator,

$$H = -t\sum_i \left(b_i^\dagger b_{i+1} + b_{i+1}^\dagger b_i\right) + \frac{U}{2}\sum_i n_i(n_i-1) + V\sum_i n_i n_{i+1}, \tag{1}$$

where b_i and $b_i^\dagger$ are the bosonic creation and annihilation operators, with algebra $[b_i, b_j^\dagger] = \delta_{ij}$, $[b_i, b_j] = 0 = [b_i^\dagger, b_j^\dagger]$, $n_i = b_i^\dagger b_i$ is the number of particles at site i, t is the hopping matrix element, and U is the on-site interaction. In the following, we will set $t = 1$ and fix the average filling $\bar{n} = 1$. Moreover, we assume the three-body constraint $(b_i^\dagger)^3 = 0$ to hold, which amounts to a truncation of the Hilbert space of each site to the three lowest occupation states 0, 1, and 2.

The model, in addition to capturing the SF-MI transition[21] characteristic of these systems for $U \gtrsim 0$, gained much attention because for nonvanishing nearest-neighbor density–density interaction $V > 0$, it also describes an HI phase, with non-trivial topological properties[3,10] and a finite nonlocal string order.

For higher values of $V > 0$, a DW phase also appears.[22,23] For moderately attractive values of $V \lesssim 0$, instead, a SF phase is expected, which was observed to turn into a PSF phase in the case of an appropriate attractive U. The ground state phase diagram is reported in Fig. 1.

The low energy effective-field theory developed in the constrained case[3] correctly captures the three insulating phases at filling $\bar{n} = 1$ in the repulsive interaction regime $U, V > 0$, as well as the SF phase for weakly attractive U. The Hamiltonian H is first mapped into a spin-1 model and then, each spin-1 variable is written as a sum of two spin-1/2, which are mapped onto two spinless fermions via Jordan Wigner transforms. A standard bosonization analysis can be applied to the resulting fermionic model, which associates bosonic fields to the two fermionic degrees of freedom (DOF) and ends up in mapping the fermionic model into two sine-Gordon Hamiltonians—decoupled in the symmetric and anti-symmetric combinations of the bosonic fields—and a coupling term negligible in the low energy limit. We refer to Ref. 3 for details of the calculation and the subsequent renormalization group analysis. In fact, in the case of fermions, the above approach was exploited exhaustively to derive a general framework for associating nonlocal string and parity order parameters to each bosonic field.[11,17] More recently,[18] it was noticed that such a procedure, when applied to the Bose–Hubbard case, provides evidence of transition to the PSF phase and its characterization, through a further nonlocal order parameter, named the odd charge parity. Here, we will prove that within the same theoretical framework, the full phase diagram of the EBH model can, in fact, be derived also at $V \geq 0$ through the appropriate nonlocal order parameters.

III. NONLOCAL ORDER PARAMETERS

The bosonization approach to the constrained EBH model[3] is associated with the symmetric (here even) bosonic field, a local representation through the parity and string operators, which can be expressed in terms of local densities n_i. The MI and HI phases were identified with the pinning of such a field to two possible distinct values, implying a finite expectation value of even parity and string operators, respectively. The previous mathematical property, in fact, signals the emergence of a hidden order, i.e., the ordering of a subset of DOF in the disordered background of the remaining DOF. In the present case of 3 DOF per site, different possible hidden orders are shown in the left panel of Fig. 1. Bosonization analysis[3,18] proves that these correspond to the finite expectation values of one or more of the following nonlocal operators:

$$O_P^{(\nu)}(j) = \prod_{i=1}^{j-1} \exp\left[i\pi\delta_\nu n_i\right], \quad \nu = e, o, \tag{2}$$

$$O_S(j) = \delta n_0 \prod_{i=1}^{j-1} \exp\left[i\pi\delta n_i\right]\delta n_j, \tag{3}$$

known as parity (O_P) and string (O_S) operators. The further index ν in the parity operator, which can be even (e) or odd (o), was introduced in Ref. 18, and corresponds to a different type of density fluctuation $\delta_\nu n_i$. Specifically,

$$\begin{aligned} \delta_e n_i &= \delta n_i \doteq n_i - 1, \\ \delta_o n_i &= n_i. \end{aligned} \tag{4}$$

First, let us discuss the parity operator. It is evident from the definition of Eq. (2) that the exponential factors assume either value $+1$ or -1, depending on δn_i on the ith site. Then, the even parity operator $O_P^{(e)}$ will maintain, on average, a finite value only when the fluctuations with respect to the background of singly occupied

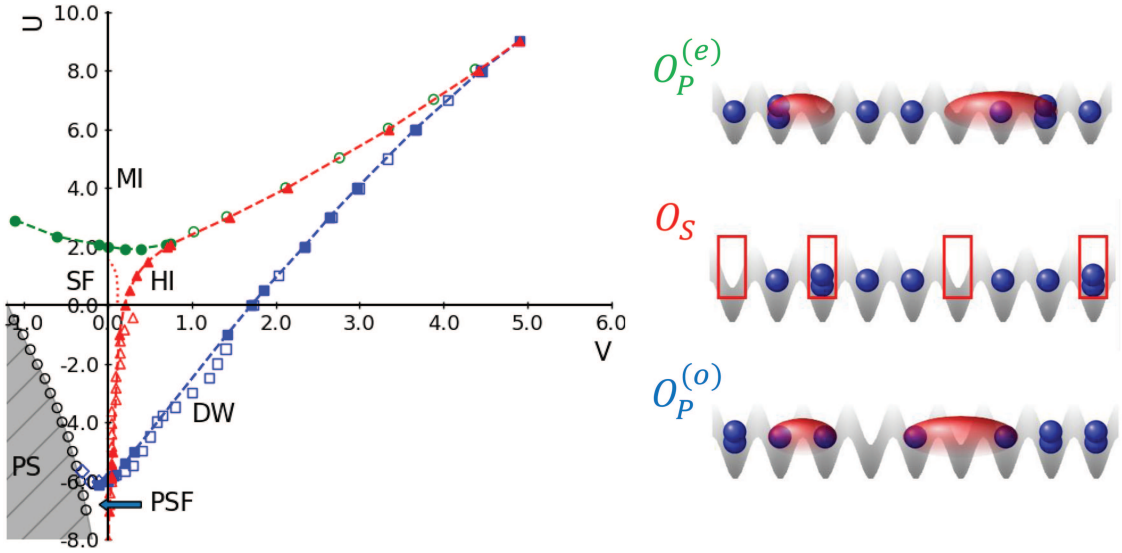

FIG. 1. Phase diagram obtained by analyzing the nonlocal operators in Eqs. (2) and (3) for three-body constrained 1D EBH model (left panel). Our results are represented by filled symbols, while the unfilled symbols correspond to the findings in Ref. 19 for a repulsive onsite interaction and in Ref. 20 for an attractive onsite interaction. The full symbols of different colors signal that the expectation value of the corresponding nonlocal operator is different from zero [green for $O_P^{(e)}$, red for O_S, and blue for $O_P^{(o)}$], separating phases with different nonlocal orders. The red dotted line close to the origin is the SF border predicted in Ref. 19. The cartoons to the right schematically represent the correlated density fluctuations underlying the possible hidden nonlocal orders. The red ellipses highlight two kinds of pairs (holon–doublon or boson–boson) with finite correlation length, which corresponds to the parity order (even or odd, respectively). The empty rectangles highlight the alternation of holons and doublons in the background of single bosons, characteristic of the string order.

sites occur in the form of correlated nearby empty (holon) and doubly occupied (doublon) pairs. Reversely, for odd parity $O_P^{(o)}$, now the background amounts to disordered holons and doublons, and fluctuations must occur in pairs of nearby singly occupied sites to maintain its expectation value finite. This is shown in the right panel of Fig. 1.

Moreover, a nonvanishing average value of the string operator O_S in Eq. (3) is obtained when holons and doublons are alternated, though diluted in the disordered single site background.

The results are summarized in Table I. Beyond the SF phase, four possible distinct phases can be obtained at filling $\bar{n} = 1$ from the ordering of the above nonlocal order parameters, according to Table I. Phases having just one nonvanishing nonlocal order (MI, HI, PSF) do not break any symmetry. The nonvanishing parameters become two in the case of the DW phase: the simultaneous presence of two nonlocal orders ends up into the genuine local order of the DW phase, which breaks the translational symmetry.

TABLE I. Summary of the expectation values of the nonlocal order parameters (NLOPs) in Eqs. (2) and (3) for each phase according to bosonization analysis.

NLOP	SF	MI	HI	PSF	DW
$O_P^{(e)}$	0	$\neq 0$	0	0	0
O_S	0	0	$\neq 0$	0	$\neq 0$
$O_P^{(o)}$	0	0	0	$\neq 0$	$\neq 0$

Also, in correspondence to each nonvanishing nonlocal order parameter, similar to what happens in the fermionic case, one or more excitation gaps are finite. In particular, we will be interested in

$$\begin{aligned} \Delta_n &= E^{(1)}(N;L) - E^{(0)}(N;L), \\ \Delta_{\alpha=1,2}(L) &= E(N+\alpha;L) + E(N-\alpha;L) - 2E(N;L), \end{aligned} \tag{5}$$

namely, the neutral gap and the single and double particle excitation gaps for N bosons on L sites. These were already used to discuss the phase diagram at $U > 0$[19,23] and $U < 0$.[20] As shall be clarified, they behave differently in different phases, but unlike the nonlocal order parameters, their finiteness cannot be used to uniquely identify all distinct phases.

IV. RESULTS

This section presents the outcomes of our analysis of the extended Bose–Hubbard model in one dimension. As mentioned earlier, the comprehensive phase diagram of this model is here inferred by evaluating the expectation values of the nonlocal operators described in Secs. I–III. To accomplish this, we represented the state using the matrix product state (MPS)[24–27] formalism and applied the Density Matrix Renormalization Group (DMRG) algorithm to ascertain the ground state.[26,28–32]

In particular, we employed the infinite DMRG algorithm[33,34] to approximate an infinite-size chain in our simulations. This approach enables us to circumvent significant issues related to the boundary effects[35] when evaluating the expectation of Eqs. (2)

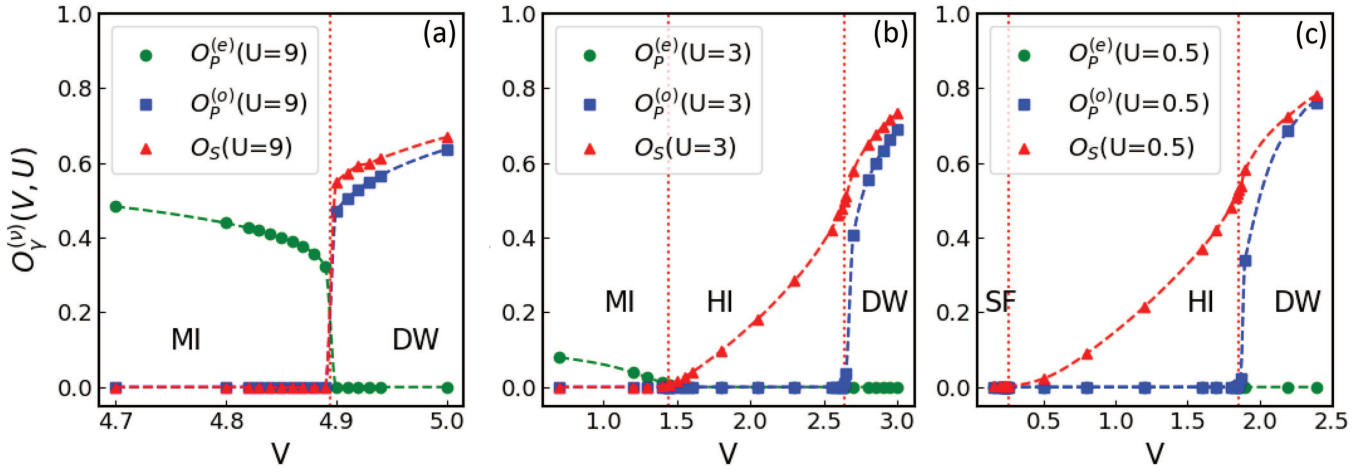

FIG. 2. The analysis of the phase diagram depicted in Fig. 1 for $U > 0$ and varying $V > 0$ reveals four different possible phases: SF, MI, HI, and DW. The three distinct scenarios are (a) Plot of the case $U = 9$; here, there is a transition from a region dominated by the even parity order (MI) to one where both string and odd parity are present (DW). (b) Plot of the case $U = 3$; here, between the two previous phases, there is a region where only the string is finite (HI). (c) Plot of the case $U = 0.5$; here, there is first a region without any order (SF), then initially only the string is finite, and finally, the odd parity also becomes greater than zero.

and (3). Moreover, there is no need for extrapolation to the thermodynamic limit, requiring fewer DMRG states for obtaining the ground state; we specifically set a maximal bond dimension of $\chi = 200$. This is enough to obtain a converged expectation value inside the phase characterized by the corresponding nonlocal order. The situation differs in computing the gaps, where the finite size algorithm is necessary.

To derive our results, we imposed a maximum limit of two bosons per site to prevent the collapse of bosons onto a single site. While this restriction alters the model's delocalization of bosons in the lattice, various phases identified in the literature for $U > 0$ remain qualitatively consistent, as illustrated for larger maximal occupation numbers ($n_{\max} = 3$ in Ref. 23 and $n_{\max} = 8$ in Ref. 36). In fact, it has been demonstrated[22] that a maximum of $n_{\max} = 5$ provides a reasonable approximation of the system (in $U > 0$ regime) without a specific limit on boson numbers.

The resulting phase diagram is presented in Fig. 1. Similar markers indicate equivalent transitions, with filled symbols representing our findings and empty symbols denoting results from the literature for the extended Bose–Hubbard model with the same three-body constraint. In addition to a region of PS in which empty and doubly occupied regions coexist, five distinct phases emerge: MI, HI, DW, SF, and PSF. Our transition points are identified where the expectation value of the operators becomes greater than zero [actually, we assume that the expectation is different from zero only when our estimate becomes greater than 3×10^{-3} for $j = 200$ in Eqs. (2) and (3)]. For the empty symbols, we are referring to Ref. 19 in the positive interaction regimes, and for negative onsite interaction, the data are taken from Ref. 20.

A. Repulsive U regime

In the region of $U > 0$, it is possible to locate the following phases: SF, MI, HI, and DW.

In order to show the different behaviors of the operators defined in Eqs. (2) and (3), it is interesting to have a look at some sections of the phase diagram. In particular, we will examine three different lines in the phase diagram, namely, $U = 9, 3,$ and 0.5.

For large onsite repulsion ($U = 9$), by increasing V from zero, one goes through a first order phase transition from an initial phase where the dominant order is captured by the even parity (MI) to one where both the odd parity and the string are greater than zero (DW), as presented in Fig. 2(a).

When the onsite interaction is reduced, for instance, to $U = 3$ as in Fig. 2(b), at sufficiently weak nearest-neighbor interaction, the even parity is the only operator different from zero: this is the MI phase. In this scenario, by further increasing the nearest-neighbor interaction, the system first enters—through a Gaussian type phase transition—a phase where the string operator is finite (HI), and then, upon an Ising type phase transition, also the odd parity becomes nonvanishing in the DW phase.

Further decreasing U toward the origin, for instance, in the case $U = 0.5$ shown in Fig. 2(c), $O_P^{(e)}$ is vanishing. At weak V, there is neither a local nor nonlocal order and the system is in the normal SF phase. By increasing V, the string parameter slowly becomes nonvanishing at the SF-HI transition. Then, by further increasing V, the odd parity also becomes different from zero and we are again in the DW phase. Even if both transitions are continuous, they belong to different universality classes. The SF-HI (and also the SF-MI) is in the Berezinskii-Kosterlitz-Thouless (BKT) universality class,[37] while the HI-DW transition is an Ising one.

In the phase diagram (Fig. 1), we compared our findings with those reported in Ref. 19 by determining the central charge.[38] Their results closely align with ours, and the two phase diagrams exhibit a significant overlap.

We also investigated the behavior of the gaps defined in Eq. (5) in this region. The results are summarized in Table II, for the

TABLE II. Gaps introduced in Eq. (5) for each phase. As explained in the text, the opening (or temporary vanishing) of the gaps supports the results obtained by the nonlocal order parameters. A null gap is intended in the thermodynamic limit.

Gap	SF	PSF	MI	HI	DW
Δ_n	0	0	$\neq 0$	$\neq 0$	$\neq 0$
Δ_1	0	$\neq 0$	$\neq 0$	$\neq 0$	$\neq 0$
Δ_2	0	0	$\neq 0$	$\neq 0$	$\neq 0$

repulsive U region as well. Since the SF phase is the only one where all gaps are zero, both SF-MI and SF-HI are signaled by any of the three gaps becoming finite. The scenario differs for other phase transitions in the region of $U > 0$ since all MI, HI, and DW phases possess a finite gap. Indeed, the transition between the distinct MI and HI phases is signaled by temporary vanishing of both charge (Δ_1 and Δ_2) and neutral (Δ_n) gaps, since the two phases are protected by different symmetries, while the transition to the latter is signaled solely by the vanishing of the neutral gap.

In the repulsive U region of the phase diagram, the gap Δ_2 provides no additional information.

B. Attractive U regime

Switching to the attractive interaction regime $U < 0$, it is possible to find the following phases: SF, PSF, HI, DW, and the PS region.

As before, let us have a look at the different behaviors of the three nonlocal operators defined in Eqs. (2) and (3). Contrarily to the case of $U > 0$, now, $O_P^{(e)}$ will be always zero and the correspondent order is absent. Thus, the phase diagram can be discussed here through the behavior of $O_P^{(o)}$ and O_S solely. We can consider two representative lines of the phase diagram, $U = -5, -6.5$, which are located above and below the transition line from the SF to PSF phase. These are shown in Fig. 3.

In particular, in (a), we consider $U = -5$: here, increasing V from zero, the system initially remains in the phase, where all nonlocal orders are zero (SF). Subsequently, similarly to the weakly repulsive U regime, first, the string O_S becomes different from zero (HI) and, then, the odd parity (DW).

Moving down to a stronger onsite attraction between bosons, in Fig. 3(b), we consider the case $U = -6.5$. Also, at weakly attractive V, a PSF phase characterized by non-null odd parity is present. Contrary to the SF phase, this phase now is partly gapped and characterized by the emergence of the hidden order identified in Ref. 18. By further increasing V, one directly enters the region in which both string and odd parity orders are finite (DW).

Also, for the $U < 0$ region, we can compare our findings with the existing results,[20] obtaining a good agreement.

Moreover, also in this region, we investigated the behavior of different gaps defined in Eq. (5). The results anticipated are given in Table II. For sufficiently weakly attractive U, the scenario is the same as for weakly repulsive U, in agreement with the phase diagram of Fig. 1. Entering the PSF phase instead, just the single particle gap opens to signal the cost in energy of adding an unpaired single particle fluctuation.[18] On the contrary, the neutral gap remains zero (for an infinite chain) since the PSF phase is still superfluid. Hence, the transition from PSF to DW is, in fact, signaled by Δ_n becoming different from zero. The same happens if instead, one moves from PSF to PS.

V. CONCLUSIONS

In summary, we presented an alternative numerical derivation of the full phase diagram of the extended Bose–Hubbard model in

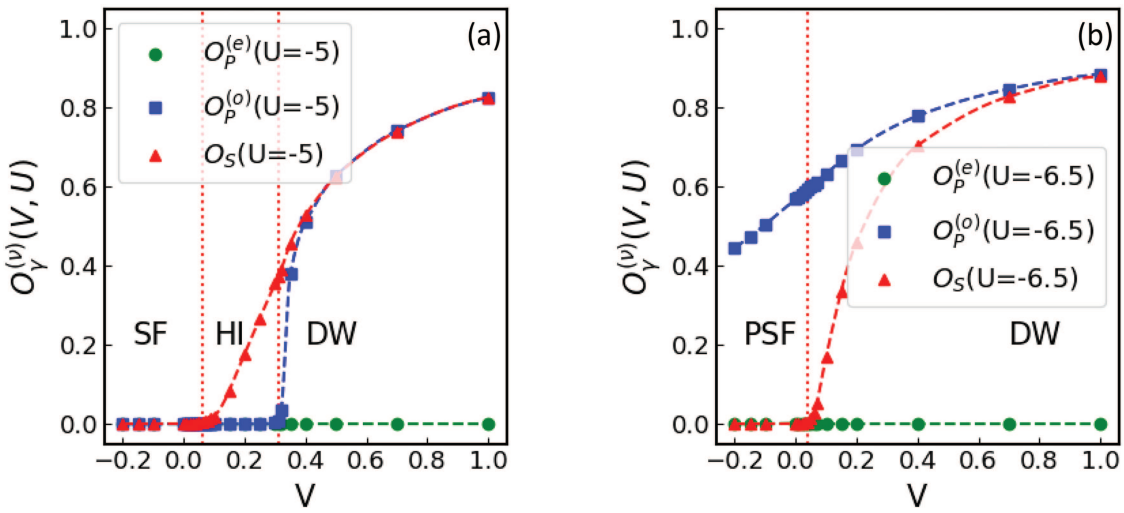

FIG. 3. The analysis of the phase diagram depicted in Fig. 1 for $U < 0$ and varying $V > 0$ reveals four different possible phases: SF, PSF, HI, and DW. The two distinct scenarios are (a) Plot of the case $U = -5$; here, there is an initial absence of order (SF). Then, the first finite operator is the string (HI), and, subsequently, the odd parity also becomes non-zero (DW). (b) Plot of the case $U = -6.5$; here, the odd parity is already greater than zero (PSF), and the transition from PSF to DW is signaled by O_S.

one dimension, which is based solely on the behavior of three nonlocal order parameters. These also amount, in addition to the string and (even) parity disorder operators introduced in Ref. 3 to describe the MI and HI insulator phases, to the odd parity operator introduced in Ref. 18 to describe the PSF phase. The latter captures the correlated fluctuations of pairs of single particles in a disordered background of holons and doublons. In addition to describing the PSF phase, the odd parity here is found to be nonvanishing also in the presence of a finite string order, describing the alternation of holons and doublons. In this case, a true local order appears, and the system enters a SSB DW phase.

The phase diagram obtained by the interplay of the three above disorder operators is shown in Fig. 1 and is in full accordance with the previous results in the literature.[19,20] Thus, our analysis is capable of characterizing distinct conducting and insulating phases of these systems by the appropriate order or disorder operator, at the same time identifying all the transition lines and the type of transition.

Notably, since the presence of nonlocal orders does not violate the Mermin–Wagner theorem, the MI, HI, and PSF nonlocal orders could persist even at nonzero temperature and can, thus, be observed in experiments with quantum matter. Another significant advantage of the identified nonlocal orders discussed here is that their measurement can be gained by just local density measures. Indeed, in the case of the MI phase, the (even) parity order was already measured in this way both in one dimension and two dimensions.[6–8] We expect that a similar result could also be obtained in the case of the odd parity characteristic of the PSF phase, which, in principle, can be generalized also to two dimensions as an odd brane parity order.[5]

ACKNOWLEDGMENTS

A.M. sincerely thanks David Campbell for introducing her several years ago to the rich physics of the extended Hubbard model and for stimulating her with his profound insights to delve into its hidden orders.

We acknowledge the financial support from the ICSC—Centro Nazionale di Ricerca in High Performance Computing, Big Data and Quantum Computing, funded by the European Union—NextGenerationEU (Grant No. CN00000013). Computational resources were provided by HPC@POLITO (http://www.hpc.polito.it). Calculations were performed using the TeNPy Library (version 0.10.0).[34]

AUTHOR DECLARATIONS

Conflict of Interest

The authors have no conflicts to disclose.

Author Contributions

Nitya Cuzzuol: Data curation (equal); Formal analysis (equal); Writing – original draft (equal); Writing – review & editing (equal). **Arianna Montorsi:** Conceptualization (lead); Funding acquisition (lead); Supervision (lead); Writing – review & editing (lead).

DATA AVAILABILITY

The data that support the findings of this study are available from the corresponding author upon reasonable request.

REFERENCES

[1] L. D. Landau, "On the theory of phase transitions. I," Zh. Eksp. Teor. Fiz. **7**, 19–32 (1937).
[2] L. D. Landau and E. M. Lifshitz, *Statistical Physics, Part 1: Course of Theoretical Physics* (Butterworth-Heinemann, Oxford, 1980), Vol. 5.
[3] E. Berg, E. G. Dalla Torre, T. Giamarchi, and E. Altman, "Rise and fall of hidden string order of lattice bosons," Phys. Rev. B **77**, 245119 (2008).
[4] A. Montorsi and M. Roncaglia, "Nonlocal order parameters for the 1D Hubbard model," Phys. Rev. Lett. **109**, 236404 (2012).
[5] S. Fazzini, F. Becca, and A. Montorsi, "Nonlocal parity order in the two-dimensional Mott insulator," Phys. Rev. Lett. **118**, 157602 (2017).
[6] M. Endres, M. Cheneau, T. Fukuhara, C. Weitenberg, P. Schauß, C. Gross, L. Mazza, M. C. Bañuls, L. Pollet, I. Bloch, and S. Kuhr, "Observation of correlated particle-hole pairs and string order in low-dimensional Mott insulators," Science **334**, 200–203 (2011).
[7] D. Wei, D. Adler, K. Srakaew, S. Agrawal, P. Weckesser, I. Bloch, and J. Zeiher, "Observation of brane parity order in programmable optical lattices," Phys. Rev. X **13**, 021042 (2023).
[8] J. Hur, W. Lee, K. Kwon, S. Huh, G. Y. Cho, and J.-Y. Choi, "Measuring nonlocal brane order with error-corrected quantum gas microscopes," Phys. Rev. X **14**, 011003 (2024).
[9] P. Sengupta, A. W. Sandvik, and D. K. Campbell, "Bond-order-wave phase and quantum phase transitions in the one-dimensional extended Hubbard model," Phys. Rev. B **65**, 155113 (2002).
[10] E. G. Dalla Torre, E. Berg, and E. Altman, "Hidden order in 1D Bose insulators," Phys. Rev. Lett. **97**, 260401 (2006).
[11] L. Barbiero, A. Montorsi, and M. Roncaglia, "How hidden orders generate gaps in one-dimensional fermionic systems," Phys. Rev. B **88**, 035109 (2013).
[12] E. Fradkin, "Disorder operators and their descendants," J. Stat. Phys. **167**, 427–461 (2017).
[13] L. F. Tocchio, F. Becca, and A. Montorsi, "Superconductivity in the Hubbard model: A hidden-order diagnostics from the Luther-Emery phase on ladders," SciPost Phys. **6**, 018 (2019).
[14] Z.-C. Gu and X.-G. Wen, "Tensor-entanglement-filtering renormalization approach and symmetry-protected topological order," Phys. Rev. B **80**, 155131 (2009).
[15] S. Fazzini, L. Barbiero, and A. Montorsi, "Interaction-induced fractionalization and topological superconductivity in the polar molecules anisotropic $t-j$ model," Phys. Rev. Lett. **122**, 106402 (2019).
[16] A. Montorsi, S. Fazzini, and L. Barbiero, "Homogeneous and domain-wall topological Haldane conductors with dressed Rydberg atoms," Phys. Rev. A **101**, 043618 (2020).
[17] A. Montorsi, F. Dolcini, R. C. Iotti, and F. Rossi, "Symmetry-protected topological phases of one-dimensional interacting fermions with spin-charge separation," Phys. Rev. B **95**, 245108 (2017).
[18] N. Cuzzuol, L. Barbiero, and A. Montorsi, "Nonlocal order parameter of pair superfluids," arXiv:2404.15972 (2024).
[19] S. Ejima, F. Lange, and H. Fehske, "Spectral and entanglement properties of the bosonic Haldane insulator," Phys. Rev. Lett. **113**, 020401 (2014).
[20] M. Dalmonte, M. Di Dio, L. Barbiero, and F. Ortolani, "Homogeneous and inhomogeneous magnetic phases of constrained dipolar bosons," Phys. Rev. B **83**, 155110 (2011).
[21] M. P. A. Fisher, P. B. Weichman, G. Grinstein, and D. S. Fisher, "Boson localization and the superfluid-insulator transition," Phys. Rev. B **40**, 546–570 (1989).
[22] T. D. Kühner, S. R. White, and H. Monien, "One-dimensional Bose-Hubbard model with nearest-neighbor interaction," Phys. Rev. B **61**, 12474–12489 (2000).
[23] D. Rossini and R. Fazio, "Phase diagram of the extended Bose–Hubbard model," New J. Phys. **14**, 065012 (2012).

[24]M. Fannes, B. Nachtergaele, and R. F. Werner, "Finitely correlated states on quantum spin chains," Commun. Math. Phys. **144**, 443–490 (1992).
[25]A. Klümper, A. Schadschneider, and J. Zittartz, "Groundstate properties of a generalized VBS-model," Z. Phys. B: Condens. Matter **87**, 281–287 (1992).
[26]S. Östlund and S. Rommer, "Thermodynamic limit of density matrix renormalization," Phys. Rev. Lett. **75**, 3537–3540 (1995).
[27]G. Vidal, "Efficient classical simulation of slightly entangled quantum computations," Phys. Rev. Lett. **91**, 147902 (2003).
[28]S. R. White, "Density matrix formulation for quantum renormalization groups," Phys. Rev. Lett. **69**, 2863–2866 (1992).
[29]S. R. White, "Density-matrix algorithms for quantum renormalization groups," Phys. Rev. B **48**, 10345–10356 (1993).
[30]J. Dukelsky, M. A. Martín-Delgado, T. Nishino, and G. Sierra, "Equivalence of the variational matrix product method and the density matrix renormalization group applied to spin chains," Europhys. Lett. **43**, 457 (1998).
[31]U. Schollwöck, "The density-matrix renormalization group," Rev. Mod. Phys. **77**, 259–315 (2005).
[32]U. Schollwöck, "The density-matrix renormalization group in the age of matrix product states," Ann. Phys. **326**, 96–192 (2011).
[33]I. P. McCulloch, "Infinite size density matrix renormalization group, revisited," arXiv:0804.2509 (2008).
[34]J. Hauschild and F. Pollmann, "Efficient numerical simulations with tensor networks: Tensor network python (TeNPy)," SciPost Phys. Lect. Notes (2018), p. 5; see https://github.com/tenpy/tenpy.
[35]C. Degli Esposti Boschi, A. Montorsi, and M. Roncaglia, "Brane parity orders in the insulating state of Hubbard ladders," Phys. Rev. B **94**, 085119 (2016).
[36]X. Deng, R. Citro, E. Orignac, A. Minguzzi, and L. Santos, "Polar bosons in one-dimensional disordered optical lattices," arXiv:1203.0505 (2013).
[37]S. Sachdev, *Quantum Phase Transitions*, 2nd ed. (Cambridge University Press, 2011).
[38]T. Giamarchi, *Quantum Physics in One Dimension* (Oxford University Press, 2003).